Biophysical Chemistry 140 (2009) 69–77

Contents lists available at ScienceDirect

Biophysical Chemistry

journal homepage: http://www.elsevier.com/locate/biophyschem

Interactions between membrane sterols and phospholipids in model mammalian and fungi cellular membranes — A Langmuir monolayer study

J. Miñones Jr. [a], S. Pais [a], J. Miñones [a], O. Conde [a], P. Dynarowicz-Łątka [b,*]

[a] University of Santiago de Compostela, Faculty of Pharmacy, Department of Physical Chemistry, Campus Sur, 15706 Santiago de Compostela, Spain
[b] Jagiellonian University, Faculty of Chemistry, Ingardena 3, 30-060 Krakow, Poland

ARTICLE INFO

Article history:
Received 16 September 2008
Received in revised form 21 November 2008
Accepted 22 November 2008
Available online 3 December 2008

Keywords:
Mixed Langmuir monolayers
Air/water interface
Phospholipid–sterol interactions

ABSTRACT

This paper is aimed at investigating sterol/phospholipid interactions in the exact proportion that occurs in fungi/mammalian cells. We have performed a thorough analysis of surface pressure (π)–area (A) isotherms with the Langmuir monolayer technique, complemented with Brewster angle microscopy (BAM) images. The following mixtures were analysed: cholesterol (Chol)–dipalmitoyl phosphatidylcholine (DPPC), Chol–dioleoyl phosphatidylcholine (DOPC), ergosterol (Erg)–DPPC, and Erg–DOPC. For each system, two different concentrations of the sterols were used, 13 and 30%, corresponding to the range of concentration found in various natural membranes.

The obtained results show the existence of attractive interactions between phospholipids and cholesterol. Mixtures with ergosterol behave quite differently, i.e. either the interactions are repulsive (mixtures with DPPC) or the system is ideal (mixtures with DOPC). The obtained results have implications in the polyene antibiotics mode of action, i.e. the polyenes may interact easier with ergosterol, present in fungi cells, as compared to cholesterol — the main sterol of the mammalian cellular membranes.

1. Introduction

The cellular membrane is not only a physical barrier separating the inside of the cell from the outside, but allows cells to selectively interact with their environment [1]. Apart from its importance in vast array of cellular processes (such as ions and metabolites transport, communication and regulation processes), it makes a site of a number of drugs acting at the membrane level of a living cell. Antimicrobial peptides, such as alamethicin [2] or gramicidin [3], polyene macrolide antibiotics (for example amphotericin B or nystatin [4]) or alkyl-lysophospholipids (a new generation anticancer drugs, like miltefosine [5] or edelfosine [6]) serve as good examples of molecules, which physiological activity occurs at lipid membrane interface. For these particular kinds of drugs, studies of their interactions with cell membranes are of utmost importance. For this purpose, several approaches are possible (reviewed in Ref. [7]). The drug–membrane interactions can be investigated with living cells or natural membranes, isolated from cells, however, due to complexity of both experimental methodology and the obtained results, such as approach is not frequent, contrary to modelling of the cellular membrane, either with lipid vesicles, bilayer lipid membranes (BLM) or Langmuir monolayers. The latter technique of monomolecular layers formed at the air/water interface has an advantage over the other methods since it allows for a continuous control of both quality of the surface and such parameters as molecular packing, physical state, lateral pressure and composition [8]. In particular, mixed Langmuir monolayers composed of constituents of biological membranes, such as phospholipids, sterols, sphingo- and glycolipids, provide a highly informative approach for studying intermolecular interactions between membrane components and biomolecules [9], and quite often can be of help in elucidating a mode of action of many physiological active compounds (see for example [10,11]).

The structural backbone of the natural membrane is a bilayer formed by phospholipids molecules, in which sterols and proteins are embedded [12]. Depending on the living organism, type of a cell and kind of a membrane, the content of phospholipids, proteins and sterols differ [13]. Also, the composition of the inner and outer layer of a membrane differs, e.g. in the outer leaflet mainly phosphatidylcholines and sphingomyelins are present, while the inner layer contains phosphatidylethanolamines and phosphatidylserines [14].

The main objective of this work was to build a model membrane of human and fungi cells in order to examine thoroughly the interactions existing between phospholipids and sterols. In fact, mixed monolayers of phospholipids and sterols, mainly cholesterol, have already been investigated [15,16], however, we are interested in a detailed study of mixed systems where the proportion of sterols to phospholipids coincides with that of natural membrane. Mammalian membranes contain high proportion of phosphatidylcholines (PC), both saturated

* Corresponding author. Tel.: +48 12 6632082; fax: +48 12 6340515.
E-mail address: ucdynaro@cyf-kr.edu.pl (P. Dynarowicz-Łątka).

0301-4622/$ – see front matter © 2008 Elsevier B.V. All rights reserved.
doi:10.1016/j.bpc.2008.11.011

and unsaturated [17]. As regards sterols, mammalian cellular membrane contains 30% of cholesterol as compared to 13% of ergosterol in fungi membrane [18]. Therefore, we have constructed model membranes containing either 13% or 30% of a sterol (ergosterol or cholesterol) and a model phospholipid (saturated: DPPC and unsaturated: DOPC). The knowledge of the interactions between phospholipids and cholesterol/ergosterol may have significant implications in the mode of action of the polyene antifungal antibiotics, which are believed to form channels in cellular membranes, due to their interactions with sterols, which are responsible for the leakage of vital cellular components, leading to the cell death [19]. Therefore, because phospholipids comprise ca. 40–50% of the cellular membrane components, their role cannot be neglected. To understand their role in the polyenes mechanism of action, it is of utmost importance to study the interactions between the antibiotic and phospholipids in the presence of sterols. Until now, the Langmuir monolayer technique was applied to examine the interactions between polyene antibiotics and either sterol [20,21] or phospholipids [22,23]. However, to understand the complex mechanism of action of the polyene antifungal it is necessary to study the interactions between the antibiotic and the lipidic components of the fungi and mammalian cellular membranes (phospholipids and sterols). However, before these kinds of studies can be performed, first the interactions existing between phospholipids and cholesterol in the very proportion they exist in natural membrane must be examined, which is the aim of this paper.

The interactions between cholesterol and phospholipids have been analysed qualitatively (by comparing the results of the experimental surface pressure–mean molecular area isotherms with the theoretical values calculated on the basis of the additivity rule) and quantitatively (from excess free energy of mixing values). In addition, we have applied modern optical method, namely Brewster angle microscopy (BAM), to visualize the structure of the investigated monolayers.

2. Experimental

The investigated sterols (cholesterol and ergosterol) as well as the investigated phospholipids (DPPC and DOPC) were supplied by *Sigma* (purity 99%). The compounds were stored in a refrigerator without the access of light. Spreading solutions were prepared by weighting a proper amount (typically 2–3 mg) of the investigated compound on the analytical balance (accurate to 0.1 mg) and dissolving each of the compound in a 4:1 mixture of chloroform:absolute ethanol (*Merck*, p. a.) in a 10 mL flask. Mixed solutions were prepared from the respective stock solutions of both compounds. The number of molecules spread on water subphase was 2.5×10^{16} molecules for DPPC–sterols mixtures and 5.6×10^{16} molecules for DOPC–sterols mixtures. Ultrapure water (produced by a Nanopure water purification system coupled to a Milli-Q water purification system, resistivity = 18.2 MΩ cm, pH = 6) was used as a subphase. The subphase temperature (20 °C) was controlled to within 0.1 °C by a circulating water system from *Haake*. Surface pressure–area isotherms were recorded with a KSV (Finland) Langmuir trough (total area = 850 cm^2), placed on an anti-vibration table. Surface pressure was measured with the accuracy of ±0.1 mN/m using a Wilhelmy plate made from platinum foil as a pressure sensor. After spreading, monolayers were left for 10 min to ensure the solvent evaporation, and afterwards the compression was initiated with a barrier speed of 15.6 $Å^2$ $molecule^{-1}$ min^{-1}.

Brewster angle microscopy images and ellipsometric measurements were performed with BAM 2 Plus (NFT, Göttingen, Germany) equipped with a 30 mW laser emitting *p*-polarized light at 532 nm wavelength which was reflected off the air/water interface at the Brewster angle (53.1°). This reflected beam passes through a focal lens, into an analyzer at a known angle of incident polarization, and finally to a CCD camera. To measure the relative thickness of the film, a camera calibration was necessary previously in order to determine the relationship between the gray level (GL) (intensity unit) and the relative reflectivity (I), according to the procedure described by Rodríguez Patino et al. [24].

The light intensity at each point in the BAM image depends on the local thickness and film optical properties. These parameters can be measured by determining the light intensity at the camera and analyzing the polarization state of the reflected light by the method based on Fresnel equations. At the Brewster angle:

$$I = |Rp|^2 = Cd^2 \quad (1)$$

where I is the relative reflectivity (defined as the ratio of the reflected intensity (I_r) and the incident intensity (I_0), $I = I_r/I_0$), Rp is the *p*-component of the light, C is a constant and d is the film thickness.

The lateral resolution of the microscope was 2 μm, the shutter speed used was 1/50 s and the images were digitalized and processed to optimize image quality; those shown below correspond to 768 × 572 pixels.

3. Results

3.1. Cholesterol–DPPC/DOPC mixtures

3.1.1. Surface pressure isotherms

Fig. 1 shows the surface pressure–area (π–A) curves for pure components (cholesterol and DPPC) and for their mixtures of $X_{chol} = 0.13$ and $X_{chol} = 0.30$. Cholesterol gives a typical condensed monolayer with a limiting area of 38 $Å^2$/molecule (estimated by extrapolation of the steep, high-pressure, linear part of the π–A curve to zero surface pressure), which is consistent with previously reported values [25–27]. Under the dynamic compression conditions applied here, the collapse pressure at 20 °C was approximately 41 mN/m. Other authors have reported similar values [26]. Once collapse occurs, the surface pressure drops to a constant value of 39 mN/m, which reflects as a plateau in the π–A isotherm. As the measured equilibrium spreading pressure obtained by us was 38 mN/m (which is in agreement with previously reported values of 36 mN/m [28] and 39.90 [29], the initial experimental collapse pressure value obtained here (41 mN/m) evidences that the monolayer in this region is in a unstable state, which is rapidly transformed into another collapsed phase that is in equilibrium with the monolayer at a lower surface pressure (39 mN/m) [30].

The physical state of the monolayer and the collapse surface pressure value can be determined in a more precise way (as compared to the π–A isotherm) with the plot of the compressional modulus (elasticity), C_s^{-1}, as a function of surface pressure (π) (Fig. 1, inset). For the investigated monolayer, C_s^{-1} values were obtained by numerical

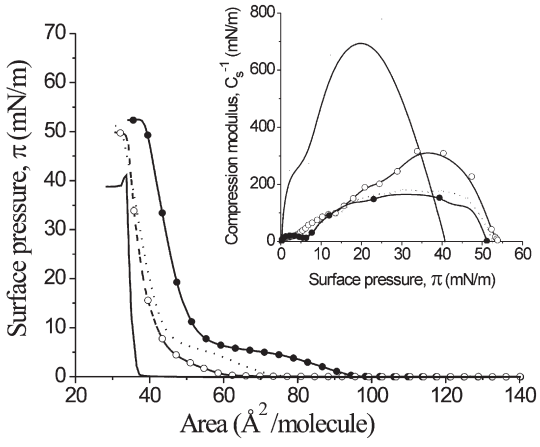

Fig. 1. Surface pressure (π)–mean molecular area (A) isotherms of cholesterol (—), DPPC (●) and their mixtures of $X_{chol} = 0.13$ (- - -) and $X_{chol} = 0.30$ (o). Subphase: water, pH = 6, T = 20 °C. Inset — the elasticity (compression modulus) values *versus* surface pressure plots for the investigated monolayers.

Table 1
Maximum compression modulus (C_s^{-1}) values for monolayers of cholesterol, DPPC and their mixtures

Monolayer	C_s^{-1} [mN/m]
Cholesterol	693
Cholesterol/DPPC, X_{chol}=0.13	310
Cholesterol/DPPC, X_{chol}=0.13	180
DPPC	164

calculation of the first derivative from the isotherm datapoints, according to the expression: $C_s^{-1}=-A(d\pi/dA)$.The highest value of the film elasticity appears as a maximum on the C_s^{-1}–π curve and the π value at which $C_s^{-1}=0$ describe the collapse surface pressure ($\pi_{collapse}$).

For cholesterol monolayer, the maximum value of C_s^{-1} (achieved at 20 mN/m) is very high, around 690 mN/m. According to Davies and Rideal [31] this value is characteristic of a very rigid structure, typical of a physical solid state. On the other hand, the π value corresponding to $C_s^{-1}=0$ ($\pi_{collapse}$) is observed with high precision in the C_s^{-1}–π curve to be 40.9 mN/m.

The monolayer of DPPC exhibits a liquid-expanded to liquid condensed (LE–LC) phase transition evidenced as a plateau in the π–A isotherm. This transition is typical of phospholipids films at temperatures below that of the gel–liquid crystal transition temperature. For DPPC this temperature is 41 °C [32]. The surface pressures at the beginning and at the end of the transition are 4.6 and 6.1 mN/m, respectively. Consequently, this is not a true first-order phase transition due to the fact that the surface pressure does not remain constant, nor it can be considered as a second order phase transition (which is characterized by the existence of a kink point in the π–A isotherm). The increase in surface pressure during the transition may be due to the fact that the film was not compressed sufficiently slowly. When the monolayer is slowly compressed (e.g. 0.8 Å^2/molecule min) on water at 18°–20°, the surface pressure values found in the literature [33,34] were 3.5–3.7 mN/m (at the beginning of the transition region) and 4.3–5.6 mN/m at the end. However, the use of faster rates of compression (15 Å^2/molecule min, or faster) leads to an increase in $\pi_{transition}$, as described elsewhere [35]. The same phenomenon occurs, even more significantly, upon increasing the temperature [36], ionic strength [37] or pH [38].

The plateau in the π–A curve of DPPC, corresponding to the above mentioned transition, reflects as a clear minimum at π=5.3 mN/m in the C_s^{-1}–π curves as shown in the inset of Fig. 1. For the mixture of X_{chol}=0.13, this minimum appears nearly at the same surface pressure,

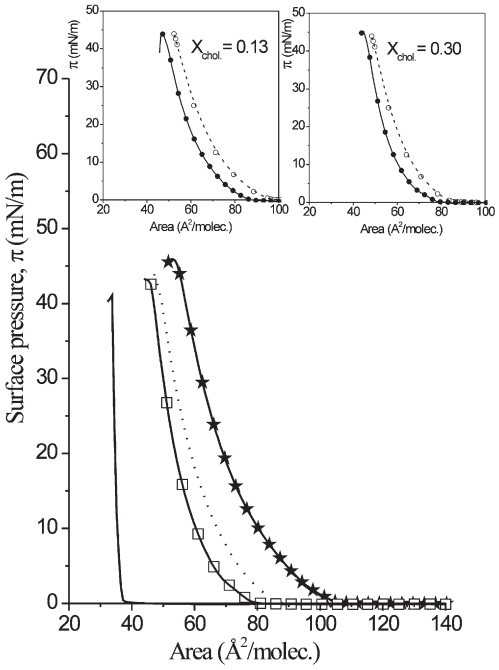

Fig. 3. Surface pressure (π)–mean molecular area (A) isotherms of cholesterol (—), DOPC (★), and their mixtures of X_{chol}=0.13 (- - -) and $X_{(Chol)}$=0.30 (□). Subphase: water, pH=6, T=20 °C. Insets — the comparison of experimental (●) and theoretical (○) isotherms.

while for the system of X_{chol}=0.30, no minimum was observed in the C_s^{-1}–π curve, indicating that no LE–LC phase transition occurs in this mixed film.

The addition of cholesterol into phospholipid monolayer causes an increase in the compressional modulus values with respect to pure DPPC film (see Table 1). This indicates that mixed cholesterol/phospholipid monolayers are more rigid as compared to pure DPPC films. This condensing effect of cholesterol on lipid monolayers is well known and has been frequently described in literature [15,21,39].

As it can be seen, the isotherms for both mixtures (X_{chol}=0.13 and X_{chol}=0.30) lie in-between those for pure components. From the results presented in Fig. 2 it can be observed that for both studied cholesterol–DPPC mixtures the experimental molecular areas are contracted in respect to theoretical values (calculated on the basis of

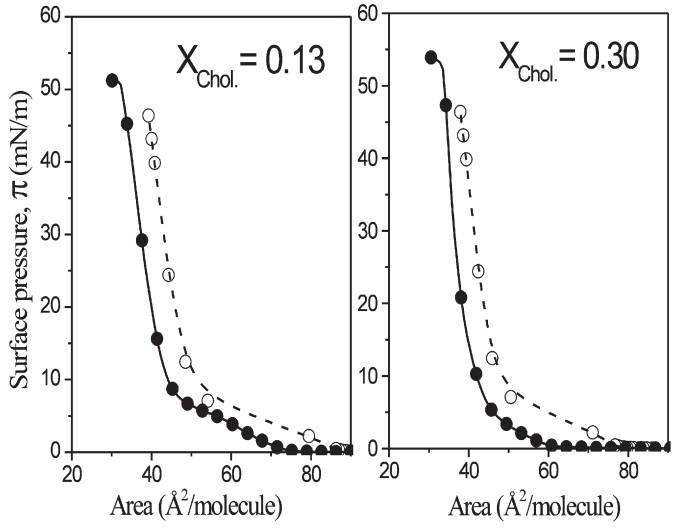

Fig. 2. The comparison of experimental (●) and theoretical (○) isotherms of cholesterol/DPPC mixtures of X_{chol}=0.13 and X_{chol}=0.30.

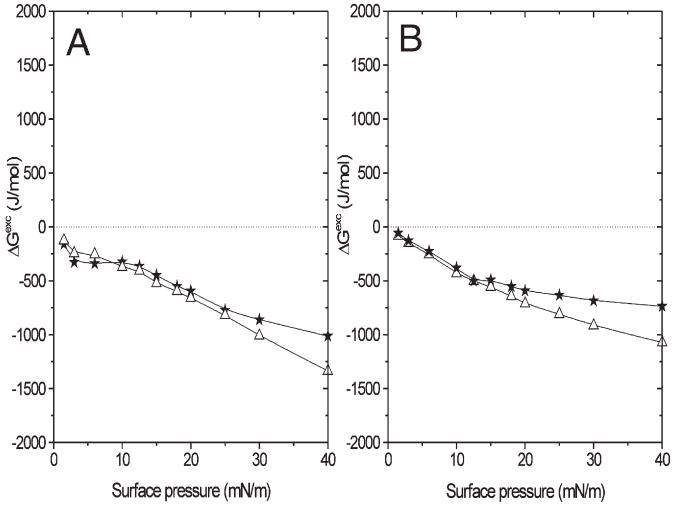

Fig. 4. The excess free energy of mixing (ΔG^{exc}) as a function of surface pressure for mixed films of cholesterol and DPPC (A) and DOPC (B). (△) $X_{(Chol)}$=0.13; (★) $X_{(Chol)}$=0.30.

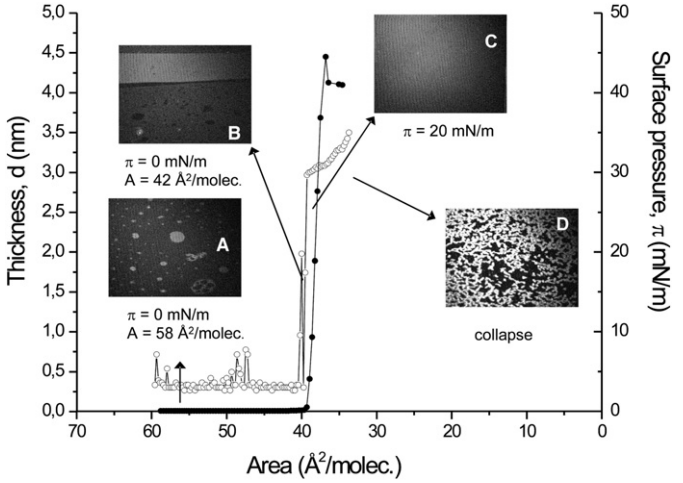

Fig. 5. The evolution of surface pressure (π) and film thickness (d) with mean molecular area (A) for cholesterol monolayer together with corresponding BAM images (see text).

the additivity rule: $A_{12}=X_1A_1+X_2A_2$). The condensing effect of cholesterol is almost of the same strength for both studied compositions with DPPC and involves the whole range of surface pressures.

Fig. 3 shows that DOPC gives a monolayer of liquid-expanded character (maximum compressibility value=130 mN/m) and the lift-off area of surface pressure is comparable to that of DPPC, however, the monolayer collapses at a lower surface pressure as compared to DPPC (46 mN/m *versus* 52.5 mN/m, respectively).

As it can be seen in this figure, mixed isotherms of cholesterol–DOPC are situated between the π/A curves for pure components, similarly to the discussed above DPPC-containing films. The comparison of theoretical and experimental isotherms (insets of Fig. 3) proves that cholesterol exerts on DOPC also a condensing effect, which indicates the existence of attractive intermolecular forces between film-forming molecules. The collapse surface pressure changes with film composition, proving the miscibility of both components in monolayers.

To get insight into the thermodynamic stability of the investigated mixed monolayers, values of the excess free energy of mixing, ΔG^{exc},

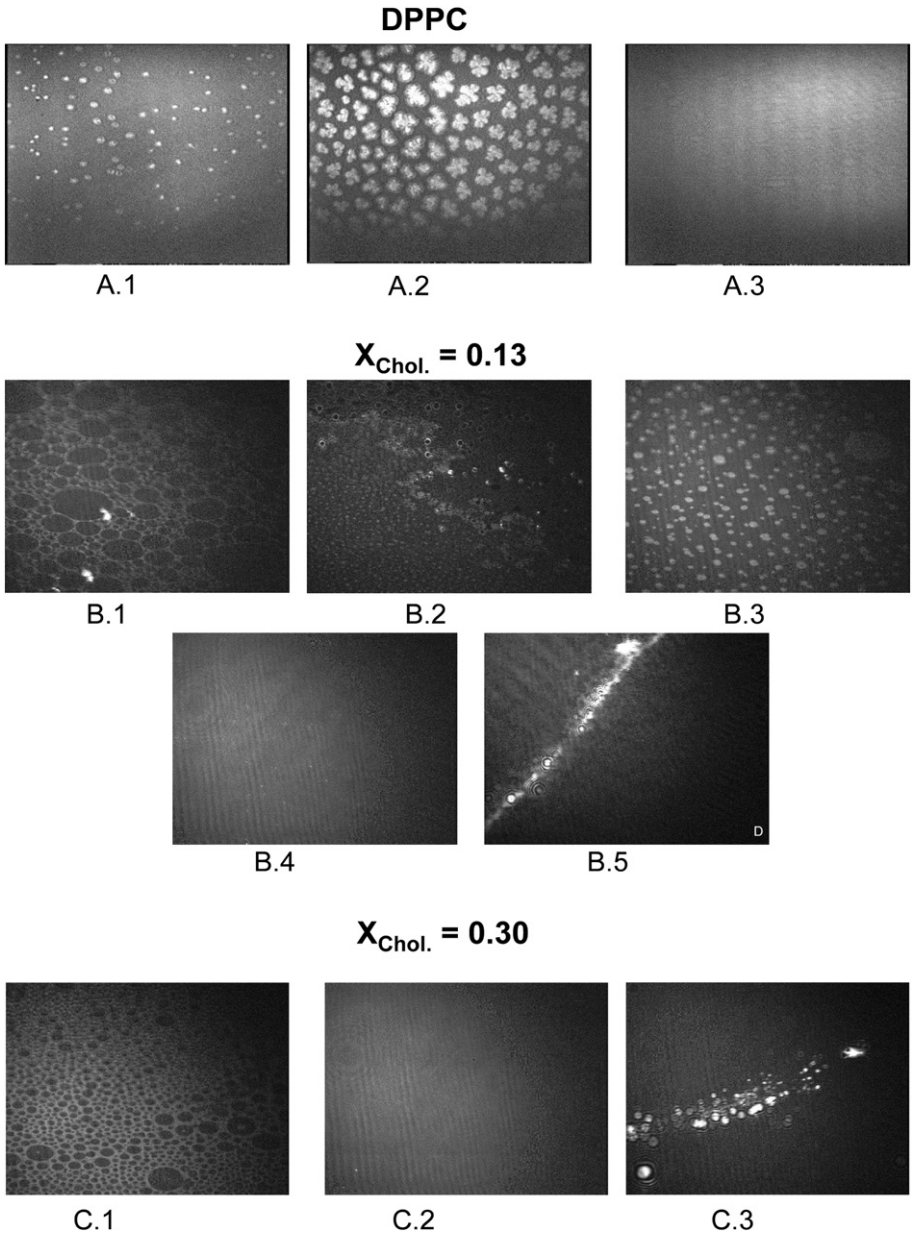

Fig. 6. BAM images of DPPC monolayer (A) and its mixed films with cholesterol of $X_{chol}=0.13$ (B) and $X_{chol}=0.30$ (C) (see text).

have been calculated from the measured π–A isotherms, using the following equation [40,41]:

$$\Delta G^{exc} = N\int_0^{\pi} A^{exc} d\pi \quad (2)$$

As it can be seen (Fig. 4A–B), the calculated values of ΔG^{exc} for cholesterol–DPPC/DOPC mixtures of both studied compositions are negative for all surface pressures, proving the existence of attractive forces between both components. Their strength is slightly stronger for cholesterol/DPPC *versus* cholesterol/DOPC mixtures. In both systems, ΔG^{exc} becomes slightly more negative as the surface pressure increases, indicating the existence of stronger interactions in more condensed monolayers. Differences between both investigated mixed films compositions (13 and 30%) are more pronounced only at higher surface pressures, where the interactions are weaker for films richer in cholesterol.

3.1.2. BAM images

3.1.2.1. Cholesterol. Fig. 5 shows BAM images for the cholesterol monolayer. Immediately after spreading of cholesterol, circular and ovoid solid domains immersed in a gaseous phase are observed. (Fig. 5A), which merge upon film compression, forming bright zones, coexisting with a gas phase (visualized in BAM as dark regions) (Fig. 5B). This gas–solid coexistence is proved in the plot of film thickness (derived from the relative reflectivity measurements), where the presence of noise peaks at low surface pressures (corresponding to the image 5 B) evidences for the presence of solid domains coexisting with the gas phase. As the film is further compressed above 20 mN/m, the monolayer becomes completely homogeneous (Fig. 5C), indicating the existence of a strongly condensed film (solid state), with the apolar groups (steroid rings) oriented toward the air. At the film collapse, a number of bright spots of 3D phase are observed.(Fig. 5D).

3.1.2.2. DPPC. The morphology of pure DPPC monolayer (Fig. 6A) at low surface pressures ($\pi \cong 0$ mN/m, 120 Å^2/molecule) evidences the existence of a homogeneous film (image not shown here), which is in concordance with the state of the in this situation: gas–liquid expanded transition. The same occurs when the monolayer is compressed to 2 mN/m, where the film exhibits a liquid expanded (LE) phase. Once the phase transition LE–LC is attained (at $\pi \cong 5$ mN/m), bright small circular and irregular domains, suspended in a darker phase, start to be formed (Fig. 6-A1). They grow along the phase transition (Fig. 6-A2), showing anisotropy as a consequence of the different tilt of DPPC alkyl chains with respect to the plane of incidence. Above the LE–LC phase transition, the domains merge

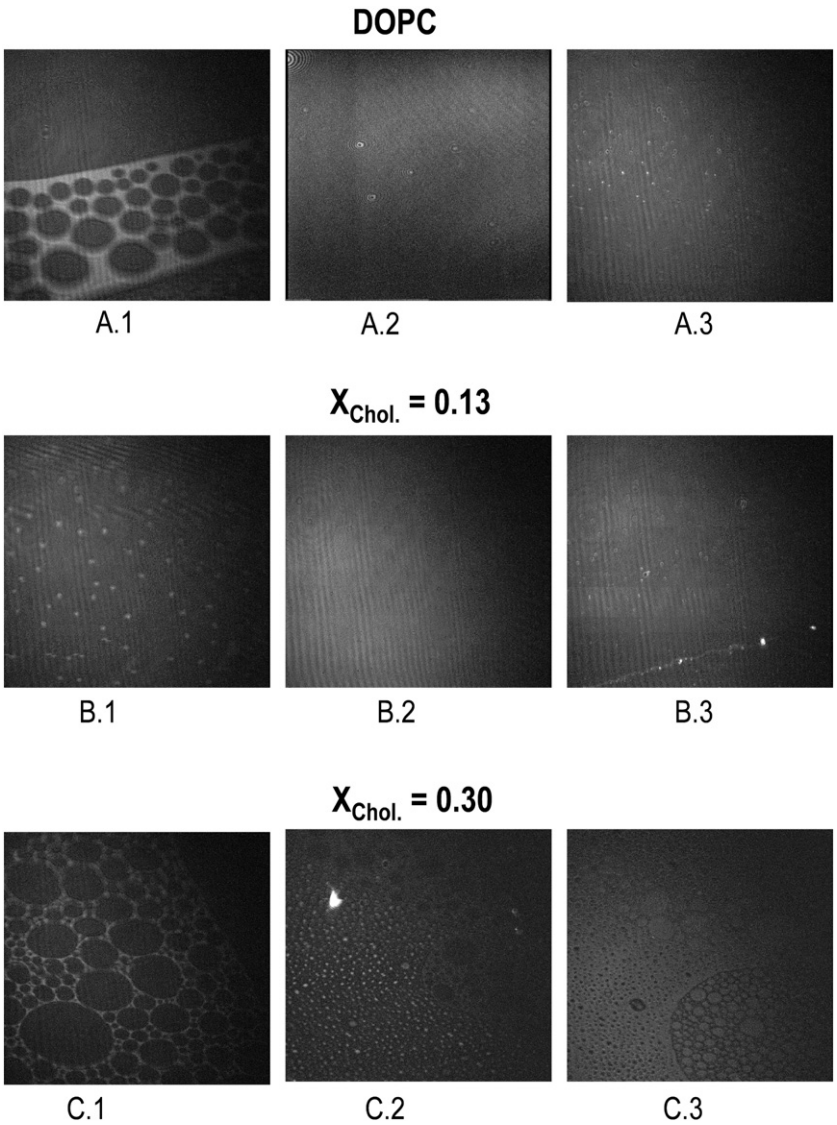

Fig. 7. Visualization of DOPC monolayer (A) and its mixed films with cholesterol of $X_{chol} = 0.13$ (B) and $X_{chol} = 0.30$ (C) by Brewster angle microscopy (see text).

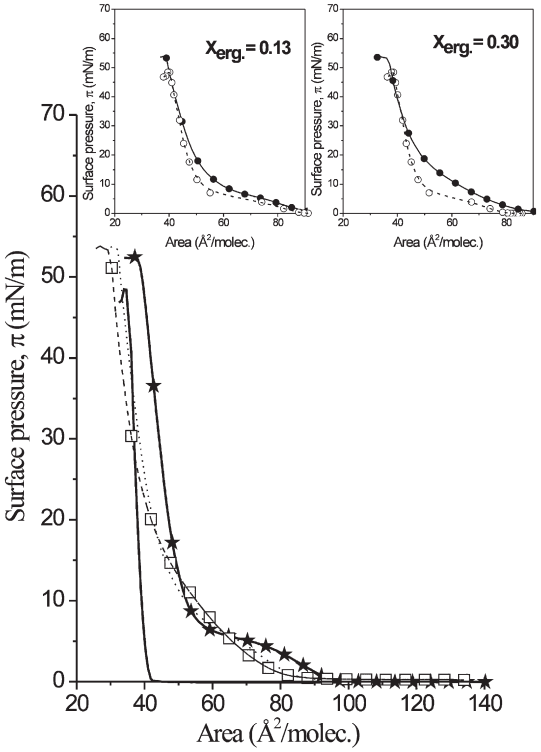

Fig. 8. Surface pressure (π)–mean molecular area (A) isotherms of ergosterol (—), DPPC (★) and their mixtures of X_{erg}=0.13 (- -) and X_{erg}=0.30 (□). Subphase: water, pH=6, T=20 °C. Insets — the comparison of experimental (●) and theoretical (○) isotherms.

together upon compression and their structure slowly blurs (Fig. 6-A3) until it disappears completely before the monolayer collapse, giving a homogeneous image (not shown).

3.1.2.3. Cholesterol–DPPC mixtures. The images corresponding to the cholesterol–DPPC mixtures of X_{chol}=0.13 are shown in Fig. 6B. In a low surface pressure region, characteristic structures of a gas–liquid expanded transition are observed (Fig. 6-B1). At the beginning of the LE–LC phase transition, small circular spots can be observed (Fig. 6-B2), which grow as the compression proceeds along this transition (Fig. 6-B3). At surface pressures above 10 mN/m, the characteristic film homogeneity of the LC phase is again observed (Fig. 6-B4), preceding the collapse of the mixed monolayer, evidenced by the formation of bright stripes (Fig. 6-B5).

For the mixed monolayer of composition X_{chol}=0.30, at the beginning of the lift-off surface pressure (π=0.1–0.5 mN/m) the coexistence of expanded phase (dark spots) dispersed in the LC zone (bright area) can be observed (Fig. 6-C1). Upon compression, the heterogeneity disappears and the image becomes homogeneous (Fig. 6-C2) until the collapse (Fig. 6-C3).

3.1.2.4. DOPC. BAM images corresponding to pure DOPC monolayer show LE–LC domains at low pressures (Fig. 7-A1). As the film is further compressed, film becomes homogeneous of liquid condensed state (Fig. 7-A2). At the collapse, few bright crystallites of 3D structure are visible.

3.1.2.5. Cholesterol–DOPC mixtures. For cholesterol/DOPC mixture of X_{chol}=0.13 (Fig. 7B) BAM images prove the existence of small, liquid-condensed domains dispersed homogeneously in the expanded phase (Fig. 7-B1). Upon compression the film becomes condensed and homogeneous (Fig. 7-B2) until the collapse, wherein the characteristic cracks are visible (Fig. 7-B3). The presence of cholesterol in the mixture causes that the domains characteristic for this sterol are indistinguishable in the mixed film. However, these domains appear for the mixture containing a higher amount of cholesterol (30%) (Fig. 7-C1). Upon film compression, the size of these domains diminishes. The image taken at the analyzer angle 0° (Fig. 7-C2) and 60° (Fig. 7-C3) prove that the domains show anisotropy due to their different inclinations. Finally they disappear at pressures close to film collapse, where the film structure becomes homogeneous (not shown).

Since no phase separation is observed for both studied mixtures until the film collapse, it is evident that cholesterol and DPPC/DOPC mix at the air/water interface in the studied compositions.

3.2. Ergosterol–DPPC mixtures

3.2.1. Surface pressure–area isotherms

The surface pressure–area isotherms for mixtures containing ergosterol and DPPC are shown in Fig. 8. As it can be seen from comparison of experimental and theoretical isotherms (Fig. 8, insets), ergosterol — contrary to cholesterol — causes an expanding effect on mixed monolayers with DPPC at lower surface pressures. The expansion is stronger for mixed monolayer richer in ergosterol. For both investigated compositions (13 and 30% of ergosterol) at higher surface pressures, above 30 mN/m, both theoretical and experimental curves coincide. This equivalence of both theoretical and experimental values at higher surface pressures suggests that under these conditions either an ideal mixed monolayer of miscible components is formed, or the film components are completely immiscible. To distinguish between these two cases the analysis of collapse surface pressures ($\pi_{collapse}$) for the mixed monolayers investigated here can be helpful. In fact, the results of Fig. 8 show that the collapse surface pressure changes with the composition of the mixed films. This is a typical behaviour of miscible components [8]. Consequently, the obtained results suggest that for the studied concentration range, DPPC is miscible with ergosterol at the air/water interface, showing an ideal behavior for X_{erg}=0.30 (at surface pressures above 30 mN/m) and exhibiting positive deviations from the additivity rule at π<30 mN/m. Positive deviations do not necessarily mean that the interactions between ergosterol and DPPC are repulsive, but that they are weaker than between like molecules (i.e. Erg–Erg; DPPC–DPPC). To get a deeper insight into this system, relative reflectivity measurements were performed upon films compression and BAM images were taken, which are described below.

3.2.2. BAM images

3.2.2.1. Ergosterol. The analysis of BAM images for mixtures with ergosterol requires the comparison with pure components as a point

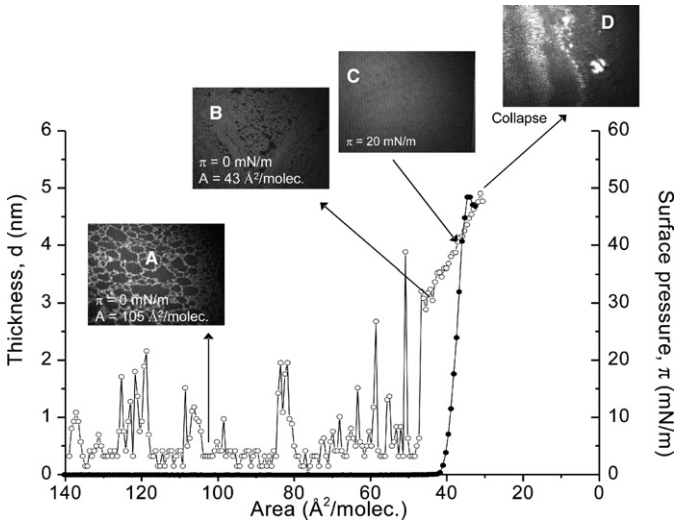

Fig. 9. Surface pressure (π) and thickness (d) *versus* mean molecular area (A) isotherm of ergosterol together with corresponding BAM images (see text).

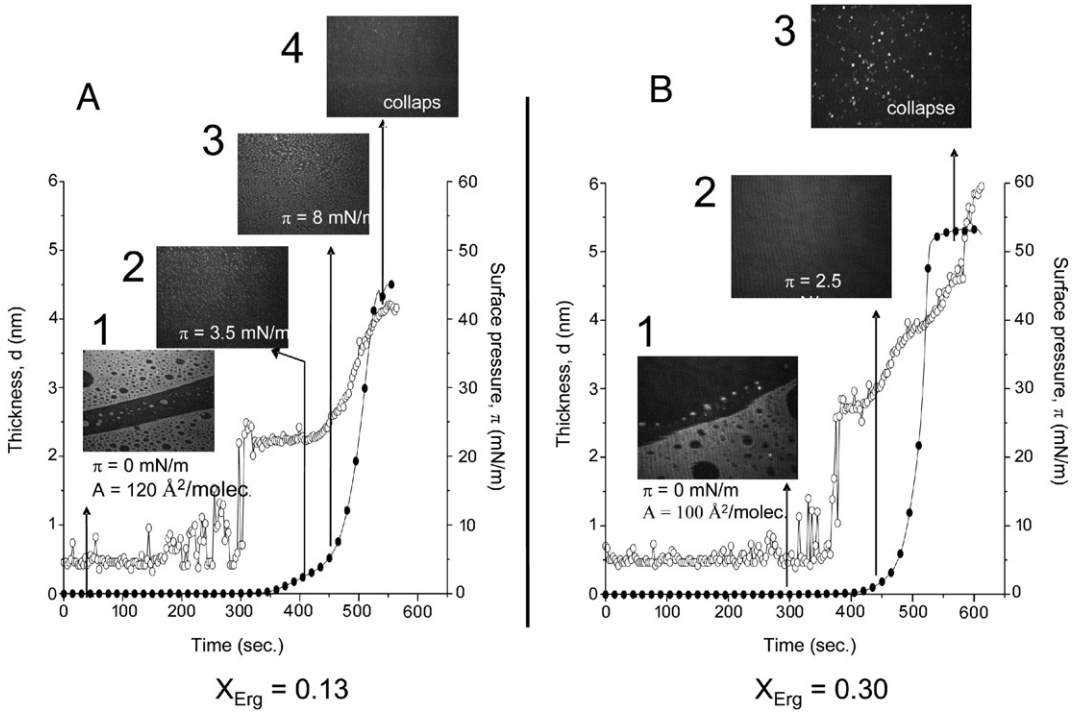

Fig. 10. The evolution of surface pressure (π) and monolayer thickness (d) with time of compression (t) for ergosterol/DPPC mixtures of X_{erg}=0.13 and X_{erg}=0.30 together with corresponding BAM images (see text).

of reference. Since the images for DPPC have already been described above, here we show photos recorded for pure ergosterol (Fig. 9). In the region of very low surface pressures ($\pi \approx 0$) (Fig. 9A) ergosterol forms irregular solid structures suspended in a homogeneous phase. This is consistent with the gas–solid phase coexistence, where low molecular density states coexist with more compact ones. These solid domains are responsible for the observed noise peaks observed in the beginning of compression on the film thickness *versus* area plot. Upon compression, solid domains merge together, forming bright zone, which cover almost the entire surface (Fig. 9B), and then the monolayer becomes homogeneous, which is characteristic of a solid state (Fig. 9C). Fig. 9D corresponds to the 3D phases involved in the collapse.

3.2.2.2. Ergosterol–DPPC mixtures. The structure of mixed monolayers containing 13% and 30% of ergosterol is very similar at surface pressures close to zero (photos 1 on Fig. 10A and B), where the characteristic domains of sterol molecules are visible. However, upon surface pressure increase, differences between both studied mixtures of different ergosterol content become clear: for the monolayer of 13%

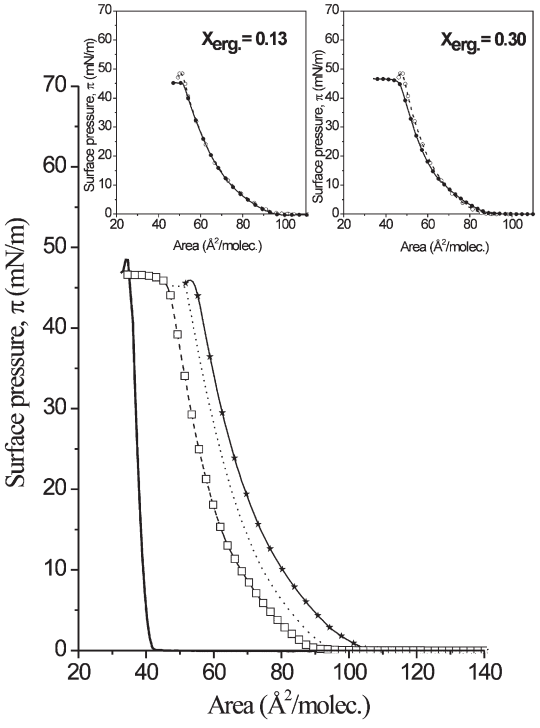

Fig. 11. Surface pressure (π)–mean molecular area (A) isotherms of ergosterol (—), DOPC (★) and their mixtures of X_{erg}=0.13 (- -) and X_{erg}=0.30 (□). Subphase: water, pH=6, T=20 °C. Insets — the comparison of experimental (●) and theoretical (○) isotherms.

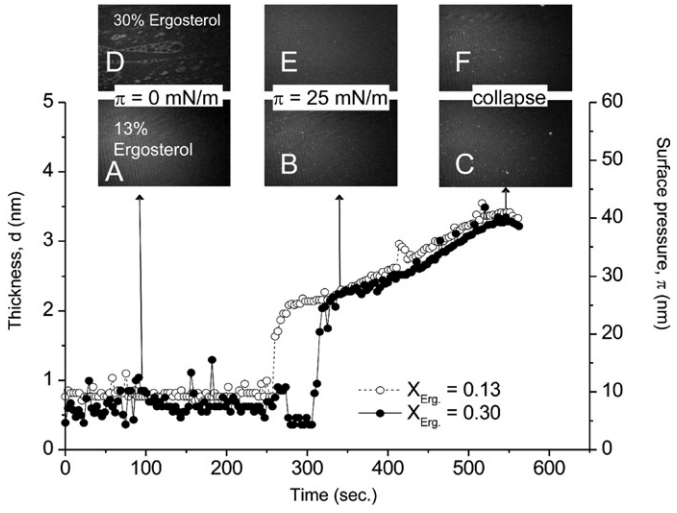

Fig. 12. The evolution of surface pressure (π) and monolayer thickness (d) with time of compression (t) for ergosterol/DOPC mixtures of X_{erg}=0.13 and X_{erg}=0.30 together with corresponding BAM images (see text).

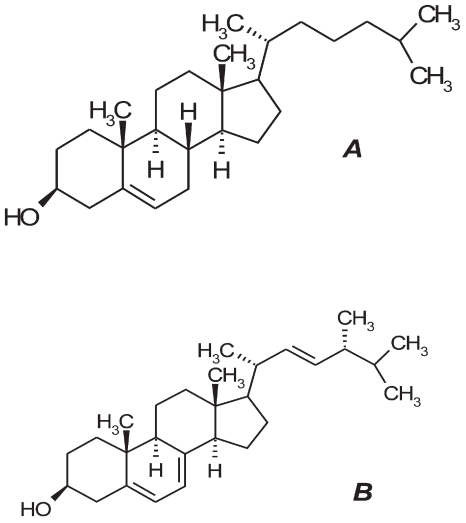

Scheme 1. Chemical structure of cholesterol (A) and ergosterol (B).

of ergosterol, a characteristic plateau of DPPC appears in the isotherm and BAM image (photos 2 and 3, Fig. 10A) show the presence of characteristic structures existing during the plateau transition of pure DPPC monolayer. The presence of the plateau is also confirmed in the film thickness curve. In contrary, this plateau does not appear for the mixture with 30% of ergosterol (homogeneous image — Fig. 10B2).

Since for both investigated mixtures with DPPC there is no evidence of phase separation, the miscibility between DPPC and ergosterol can be assured.

3.3. Ergosterol–DOPC mixtures

3.3.1. Surface pressure–area isotherms

The pressure–area isotherms are shown in Fig. 11. The isotherms for mixtures are situated between those for pure components. As evidenced in the insets, experimental and theoretical curves nearly coincide for both studied compositions. Therefore, the system either behaves ideally, or there is a phase separation. In order to distinguish between these two possibilities, the films were visualized with BAM.

3.3.2. BAM images

Mixtures with DOPC containing 13% of ergosterol at $\pi = 0$ mN/m are homogeneous (Fig. 12A) and this does not change upon compression (Fig. 12B) until the collapse, where small bright 3D structures appear (Fig. 12C). Mixture containing higher proportion of ergosterol exhibits typical ergosterol structures at large molecular areas (Fig. 12D), however, later on the film becomes homogeneous (Fig. 12E) and finally collapses (Fig. 12F). The film thickness measurements upon compression for both mixtures have a very similar course and no phase separation between DOPC and ergosterol is observed, which proves that these mixtures behave ideally.

4. Discussion

Both investigated phosphatidylcholines (DPPC and DOPC) were found to interact differently with the studied sterols, i.e. while in mixtures with cholesterol always contractions (attractive intermolecular interactions) are observed, films containing ergosterol either show expansion or behave ideally. Such a different behavior can be due to differences in the chemical structure of cholesterol and ergosterol. Namely, ergosterol possesses two additional double bonds (one in the side chain and another one in the sterol ring) as well as an additional methyl group in the side chain as compared to cholesterol (Scheme 1). Especially the presence of an unsaturated bond in the hydrocarbon chain makes the molecule more rigid and more resistant to conformational changes [42]. As a result, the accommodation of phospholipids molecules between ergosterol molecules is more difficult *versus* cholesterol and therefore the condensing effect of cholesterol on phospholipids is higher than that of ergosterol. Anyway, both phospholipids form miscible systems with both sterols, but as regards ergosterol, there are differences regarding the kind of a phospholipid. BAM images together with π–A isotherms clearly indicate that ergosterol mixes ideally with DOPC. The situation, however, is different for DPPC. The observed positive deviations from ideality at low pressures evidence for interactions between molecules.

The above results are important in understanding the effect of phospholipids on the interactions between membrane sterols and polyene antibiotics, especially amphotericin B.

It is known that the site of action of polyene antibiotics is the cellular membrane and the antibiotic/sterol interactions are crucial for polyenes activity. Moreover, the similarity between fungi and mammalian membrane (both contain sterols) is responsible for the toxicity of these drugs. Although the presence of sterols in a membrane is believed to be required for polyenes activity, the interactions with other membrane components, especially phospholipids, must also be taken into account since the sterols are always associated with phospholipids in natural membranes.

Mixtures with cholesterol (especially these of $X_{chol} = 0.3$) mimic the mammalians cellular membrane. Since both components were found to mix and interact, the effective concentration of unbound cholesterol molecules, capable of interacting with the polyene, is lowered. This means that the antibiotic molecules have to compete with phospholipids to be able to interact with cholesterol and form pores. In this way, the toxicity of the antibiotic towards human cells is decreased.

Mixtures with ergosterol (especially these of $X_{erg} = 0.13$) mimic fungi cellular membrane. Very weak repulsive interactions (for DPPC) or ideality (for DOPC) observed in these mixtures prove that the whole amount of ergosterol is unbound with membrane phospholipids, i.e. can easily interact with the antibiotic, and form channels (pores) in fungi cellular membrane. This explains the observed toxicity of polyenes towards fungi.

The obtained results indicate that amphotericin B in cellular membranes (because of different interactions between phospholipids and cholesterol/ergosterol) can interact much easier with ergosterol as compared to cholesterol. This explains the fact that the affinity of the antibiotic or its derivatives towards ergosterol was found to be higher as compared to cholesterol [18,21,43,44].

Acknowledgements

The authors acknowledge the support of the Ministerio de Educación y Ciencia (Spain),through the Project I+D, number CTQ2005-01861.

References

[1] D. Chapman, Biological Membranes — Physical Fact and Function, Academic Press, London, 1968, p. 7.
[2] B. Becingen, Structure and functions of channel-forming peptides: magainins, cecropins, melittin and alamethicin, J. Membr. Biol. 156 (1997) 197–211.
[3] B. Corry, S.H. Cung, Mechanism of valence selectivity in biological ion-channels, Cell. Mol. Life Sci. 63 (2006) 301–315.
[4] S.B. Zotchev, Polyene macrolide antibiotics and their application in human therapy, Curr. Med. Chem. 10 (2003) 211–223.
[5] B. More, H. Bhatt, V. Kukreja, S.S. Ainapure, Miltefosine— great expectations against visceral leishmaniasis, J. Postgrad. Med. 49 (2003) 101–103.
[6] C. Gajate, F. Mollinedo, Biological activities, mechanism of action and biomedical prospects of the antitumor ether phospholipid ET-18-OCH3 (edelfosine), a proapoptotic agent in tumor cells, Curr. Drug Metab. 3 (2002) 491–525.
[7] R. Maget-Dana, The monolayer technique: a potent tool for studying the interfacial properties of antimicrobial and membrane-lytic peptides and their interactions with lipid membranes, Biochim. Biophys. Acta 1462 (1999) 109–140.
[8] G.L. Gaines, Insoluble Monolayers at the Liquid–Gas Interfaces, Interscience, New York, 1966.

[9] D. Cadenhead, Structure and properties of cell membranes, in: G. Benga (Ed.), Monomolecular Films as Biomembrane Models, vol. 3, CRC Press, Boca Raton, FL, 1985, p. 21.
[10] K. Hąc-Wydro, P. Dynarowicz-Łątka, Interaction between nystatin and natural membrane lipids in Langmuir monolayers — the role of a phospholipid in the mechanism of polyenes mode of action, Biophys. Chem. 123 (2006) 154–161.
[11] K. Hąc-Wydro, P. Wydro, P. Dynarowicz-Łątka, Interactions between dialkyldimethylammonium bromides (DXDAB) and sterols — a monolayer study, J. Colloid Interface Sci. 286 (2005) 504–510.
[12] S.J. Singer, G.L. Nicolson, The fluid mosaic model of the structure of cell membranes, Science 175 (1972) 720–731.
[13] G. Karp, Cell and Molecular Biology: Concepts and Experiments, Wiley and Sons, New York, 2004 Chapter 4.
[14] J.A.F. Op den Kamp, Lipid asymmetry in membranes, Annu. Rev. Biochem. 48 (1979) 47–71.
[15] K. Gong, S.S. Feng, M.L. Go, P.H. Soew, Effects of pH on the stability and compressibility of DPPC/cholesterol monolayers at the air–water interface, Colloids Surf. A 207 (2002) 113–125.
[16] P. Dynarowicz-Łątka, K. Hąc, Interactions between phosphatidylcholines and cholesterol in monolayers at the air/water interface, Colloids Surf. B 37 (2004) 21–25.
[17] M.I. Guirr, A.T. James, Lipid Biochemistry, University Press, Cambridge, 1980.
[18] J. Barwicz, P. Tancrede, The effect of aggregation state of amphotericin-B on its interactions with cholesterol- or ergosterol-containing phosphatidylcholine monolayers, Chem. Phys. Lipids 85 (1997) 145–155.
[19] B. de Kruijf, R.A. Demel, Polyene antibiotic–sterol interactions in membranes of *Acholeplasma laidlawii* cells and lecithin liposomes. 3. Molecular structure of the polyene antibiotic–cholesterol complexes, Biochim. Biophys. Acta 339 (1974) 57–70.
[20] R. Seoane, J. Miñones, O. Conde, E. Iribarnegaray, M. Casas, Interactions between amphotericin-B and sterols in monolayers. Mixed films of amphotericin B–cholesterol, Langmuir 15 (1999) 5567–5573.
[21] R. Seoane, J. Miñones, O. Conde, M. Casas, E. Iribarnegaray, Interaction between amphotericin B and sterols in monolayers. Mixed Films of ergosterol–amphotericin B, Langmuir 15 (1999) 3570–3573.
[22] J. Miñones Jr, J. Miñones, O. Conde, M.A. Rodriguez Patino, P. Dynarowicz-Łątka, Mixed monolayers of amphotericin B–dipalmitoyl phosphatidyl choline: study of complex formation, Langmuir 18 (2002) 2817–2827.
[23] J. Miñones Jr., P. Dynarowicz-Łątka, O. Conde, J. Miñones, E. Iribarnegaray, M. Casas, Interactions of amphotericin B with saturated and unsaturated phosphatidylcholines at the air/water interface, Colloids Surf. B 29 (2003) 205–215.
[24] J.M. Rodríguez Patino, C.C. Sánchez, N.R. Rodríguez Niño, Morphological and structural characteristics of monoglyceride monolayers at the air–water interface observed by Brewster angle microscopy, Langmuir 15 (1999) 2484–2492.
[25] R. Seoane, J. Miñones, O. Conde, J. Miñones Jr., M. Casas, E. Iribarnegaray, Thermodynamic and Brewster angle microscopy studies of fatty acid/cholesterol mixtures at the air/water interface, J. Phys. Chem. B 104 (2000) 7735–7744.
[26] E. Takano, Y. Ishida, M. Iwahashi, T. Araki, K. Iryama, Surface chemical and morphological study on monolayers of cholesterol, cholestanol, and their derivatives conjugated, Langmuir 13 (1997) 5782–5786.
[27] P. Baglioni, G. Cestelli, L. Dei, G. Gabrielli, Monolayers of cholesterol at water–air interface: mechanism of collapse, J. Colloid Interface Sci. 104 (1985) 143–150.
[28] M.C. Phillips, H. Hauser, Spreading of solid glycerides and phospholipids at the air/water interface, J. Colloid Interface Sci. 49 (1974) 31–39.
[29] K. Tajima, N.L. Gershfeld, Equilibrium studies of lecithin–cholesterol interactions. II. Phase relations in surface films: analysis of the "condensing" effect of cholesterol, Biophys. J. 22 (1978) 489–500.
[30] A.F.M. Snick, A.J. Kruger, P.J. Joos, J. Colloid Interface Sci. 66 (1978) 435.
[31] J.T. Davies, E.K. Rideal, Interfacial Phenomena, Academic Press, New York, 1963, p. 265.
[32] L.W. Horn, N.L. Gershfeld, Equilibrium and metastable states in lecithin films, Biophys. J. 18 (1977) 301–310.
[33] M. Matsumoto, Y. Tsujii, K.I. Nakamura, T. Yoshimoto, A trough with radial compression for studies of monolayers and fabrication of Langmuir–Blodgett films, Thin Solid Films 280 (1996) 238–243.
[34] C.W. McConlogue, D. Malamud, T.K. Vanderlick, Interaction of DPPC monolayers with soluble surfactants: electrostatic effects of membrane perturbants, Biochim. Biophys. Acta 1372 (1998) 124.
[35] V. Vie, N. Van Mau, E. Lesniewska, J.P. Goudonnet, F. Heitz, C. Legrimellec, Distribution of ganglioside G(M1) between two-component, two-phase phosphatidylcholine monolayers, Langmuir 14 (1998) 4574–4583.
[36] T.H. Chou, C.H. Chang, Thermodynamic characteristics of mixed DPPC/DHDP monolayers on water and phosphate buffer subphases, Langmuir 16 (2000) 3383–3390.
[37] A. Tronin, V. Shapovalov, Ellipsometric model for two-dimensional phase transition in Langmuir monolayers, Thin Solid Films 312 (1998) 785–789.
[38] B.M. Discher, W.R. Schief, V. Vogel, S.B. Hall, Phase separation in monolayers of pulmonary surfactant phospholipids at the air–water interface: composition and structure, Biophys. J. 77 (1999) 2851–2861.
[39] J. Miñones Jr., I. Rey Gómez-Serranillos, O. Conde, P. Dynarowicz-Łątka, J. Miñones, J. Colloid Interface Sci. 301 (2006) 258.
[40] F.C. Goodrich, Proceedings of the Second International Congress on Surface Activity, Butterworth, London, 1957, p. 85.
[41] R.E. Pagano, N.L. Gershweld, A millidyne film balance for measuring intermolecular energies in lipid films, J. Colloid Interface Sci. 41 (1972) 311–317.
[42] M. Bagiński, A. Tempeczyk, E. Borowski, Comparative conformational analysis of cholesterol and ergosterol by molecular mechanism, Eur. Biophys. J. 17 (1989) 159.
[43] K. Hac_Wydro, P. Dynarowicz-Łątka, J. Gzybowska, E. Borowski, Interactions of amphotericin B derivative of low toxicity with biological membrane components. The Langmuir monolayer approach, Biophys. Chemist. 116 (2005) 77.
[44] J. Miñones Jr., O. Conde, P. Dynarowicz-Łątka, M. Casas, Penetration of amphotericin B into DOPC monolayers containing sterols of cellular membranes, Colloids Surf. A 270 (2005) 129.